

Stress-based elastic anisotropic unilateral degradation model for concrete

J. Y. Wu

Department of Civil Engineering, South China University of Technology, Guangzhou, China

J. Li

Department of Building Engineering, Tongji University, Shanghai, China

ABSTRACT: In this paper a thermodynamically consistent stress-based elastic anisotropic degradation unilateral model is proposed and then applied to concrete modeling. The increases of the intrinsic secant compliances cumulated under purely positive and purely negative stresses are adopted as the internal variables, and therefore the hypothesis of strain equivalence or strain energy equivalence is no longer required. To describe the unilateral effects, the new *consistent* positive and negative projection operators are proposed, and the secant constitutive law is then established within the framework of irreversible thermodynamics. The rate formulations and the corresponding tangent stiffness are also derived, which can be employed to develop standard structure of the classical multisurface return mapping integration algorithm. Finally, the proposed model is verified by application to concrete modeling.

1 INTRODUCTION

For quasi-brittle geomaterials such as concrete, rock, ceramics, etc., it is reasonable to assume that in the virgin undamaged material the distribution of microdefects is isotropic. However, due to the irreversible growth of the microdefects dominantly in the direction perpendicular to the maximum tensile stress (Krajcinovic 2003), this isotropy will be destroyed during the loading history, which is generally referred to as damage induced anisotropy and plays a crucial role in the constitutive modeling.

Attributed to the pioneering work of Kachanov (1958), continuum damage mechanics (CDM) and its coupling with plasticity have become a powerful tool in the constitutive modeling of many engineering materials. From the physically motivated viewpoint, the damage is directly characterized as the degradation of the stiffness or the increase of the compliance. Therefore, the so-called elastic or inelastic anisotropic degradation model which introduces the degradation strain rate (Hueckel & Maier 1977) due to the degradation of secant stiffness, was preferred in the modeling of anisotropic damage and might be the most widely adopted method in the literature.

In Ortiz (1985) an inelastic anisotropic degradation model was systematically proposed, in which the remarkable limitation was that the damages due to tensile and compressive stresses were controlled by a single cumulated damage variable. The above

anisotropic degradation model was later developed by others (Simo & Ju 1987, Ju 1989, Yazdani & Schreyer 1990, Neilsen & Schreyer 1992, Govindjee et al. 1995, Meschke et al. 1998, etc.). Carol et al. (1994) summarized the plastic-like framework of elastic degradation, and later in Carol et al. (2001) an elastic orthotropic degradation model was proposed based on the hypothesis of strain energy equivalence (Cordebois & Sidoroff 1979). The above orthotropic degradation model was further improved in Hansen et al. (2001) by employing plasticity to describe the unilateral effects and the nonlinear performances under compressive stresses, however, the accompanied stiffness degradation still could not be considered.

Despite the above substantial and noteworthy contributions, the modeling of anisotropic degradation still remains a challenging issue, among which the key unsolved problem is the consistent description of the unilateral effects that is of great significance in the nonlinear analysis of concrete (Mazars et al. 1990) under cyclic loading history. In all the degradation models considering the unilateral effects, none of the employed projection operators are thermodynamically consistent in the sense of non-zero energy dissipations or generations upon fixed damage (Carol & Willam 1996). Furthermore, developing the concerned implicit numerical integration method is almost impossible and the time-consuming explicit numerical integration scheme has to be employed. It was

not until recently, the implicit integration method for the Ortiz's model was suggested in Mahnken et al. (2000); however, the derivations were rather complex and the final expressions were terribly lengthy, which heavily restrains its popularity.

Noticing the above facts, in this contribution a thermodynamically consistent stress-based elastic anisotropic degradation unilateral model is proposed and then applied to concrete modeling. The increases of the intrinsic secant compliance under the purely positive and purely negative stresses are adopted as the internal damage variables, and the generally adopted hypothesis of strain equivalence (Lemaitre 1971) or strain energy equivalence (Cordebois & Sidoroff 1979) is no longer required. To consider the unilateral effects, new *consistent* positive and negative projection operators are proposed, and the secant constitutive law is then established within the framework of irreversible thermodynamics. The rate formulations and the corresponding tangent stiffness are also derived, which can be employed to develop a standard structure of the classical multisurface return mapping integration algorithm. Finally the proposed model is partially verified by application to concrete.

2 GENERAL FORMULATIONS

2.1 Elastic degradation model

To avoid distracting, from now on we pay our attentions only on the cases in absent of irreversible deformations which can generally be considered by the coupling of plasticity. As is known, for an initially isotropic material the undamaged compliance \mathbf{C}_0 and stiffness \mathbf{S}_0 respectively read as two constant fourth-order symmetric isotropic tensors, i.e.

$$\mathbf{C}_0 = \frac{1}{E_0} \left[(1 + \nu_0) \mathbf{I} \otimes \mathbf{I} - \nu_0 \mathbf{I} \otimes \mathbf{I} \right], \quad \mathbf{S}_0 = \mathbf{C}_0^{-1} \quad (1)$$

where E_0 and ν_0 respectively denote the Young's modulus and the Poisson's ratio, and \mathbf{I} signifies the second-order identity tensor. Once damaged, the material secant compliance \mathbf{C} will increase and, the secant stiffness \mathbf{S} will be degraded, i.e.

$$\mathbf{C} = \mathbf{C}_0 + \mathbf{\Lambda}, \quad \mathbf{S} = \mathbf{C}^{-1}, \quad \mathbf{C} : \mathbf{S} = \mathbf{I} \quad (2)$$

where, $\mathbf{\Lambda}$ signifies the increased secant compliance due to the damage (microvoids or microvoids) evolution. For an elastic degradation material, the unloading path always linearly points to the origin, and during the unloading-reloading histories the material compliance (or stiffness) remains constant and equal to its current secant value.

For the classical Green elastic (or hyperelastic) material, there exists a well-defined energy potential. Correspondingly, the Gibbs free energy ψ depends on

the current stress and the damage states. Under such circumstance, ψ is generally assumed as

$$\psi = \frac{1}{2} \boldsymbol{\sigma} : \mathbf{C} : \boldsymbol{\sigma} = \frac{1}{2} \boldsymbol{\sigma} : \mathbf{C}_0 : \boldsymbol{\sigma} + \frac{1}{2} \boldsymbol{\sigma} : \mathbf{\Lambda} : \boldsymbol{\sigma} \quad (3)$$

Confining the attention to the purely mechanical process, the Clausius-Duhem inequality takes the form

$$\dot{\psi} - \boldsymbol{\epsilon} : \dot{\boldsymbol{\sigma}} \geq 0 \quad (4)$$

for any admissible process. By taking the time derivatives of Equation 3, substituting into Equation 4, one obtains the stress-strain relation as follows

$$\boldsymbol{\epsilon} = \frac{\partial \psi}{\partial \boldsymbol{\sigma}} = \mathbf{C} : \boldsymbol{\sigma}, \quad \boldsymbol{\sigma} = \mathbf{S} : \boldsymbol{\epsilon} \quad (5)$$

2.2 Degradation strain

The rate form of constitutive relation can then be obtained from Equation 5 as

$$\dot{\boldsymbol{\epsilon}} = \mathbf{C} : \dot{\boldsymbol{\sigma}} + \dot{\mathbf{C}} : \boldsymbol{\sigma} = \boldsymbol{\epsilon}^r + \boldsymbol{\epsilon}^d \quad (6)$$

$$\dot{\boldsymbol{\sigma}} = \mathbf{S} : \dot{\boldsymbol{\epsilon}} + \dot{\mathbf{S}} : \boldsymbol{\epsilon} = \mathbf{S} : (\dot{\boldsymbol{\epsilon}} - \dot{\boldsymbol{\epsilon}}^d) = \mathbf{S} : \dot{\boldsymbol{\epsilon}}^r \quad (7)$$

where the relations $\dot{\mathbf{S}} = -\mathbf{S} : \dot{\mathbf{C}} : \mathbf{S}$ from the time derivatives of Equation 2₍₃₎ are called for in the above derivations. In Equations 6 and 7, $\dot{\boldsymbol{\epsilon}}^r$ is the resisting strain rate that would be obtained by preventing the microcracks from evolution further, and $\dot{\boldsymbol{\epsilon}}^d$ denotes the degradation strain rate due to the increase of secant compliance (or degradation of the secant stiffness), respectively with the following expressions

$$\dot{\boldsymbol{\epsilon}}^r = \mathbf{C} : \dot{\boldsymbol{\sigma}}, \quad \dot{\boldsymbol{\epsilon}}^d = \dot{\mathbf{C}} : \boldsymbol{\sigma} \quad (8)$$

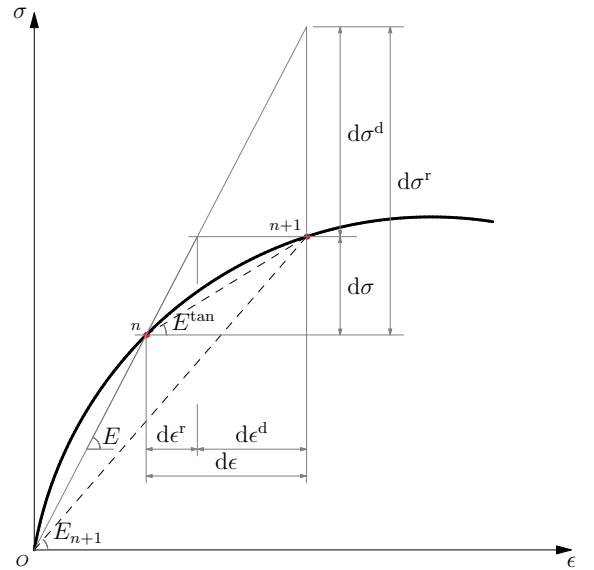


Figure 1: Definitions of the degradation strain and resisting strain rates under 1-D stress.

The above defined resisting and degradation components of the strain rate can be referred to Figure

1, where the 1-D stress-strain diagram in terms of a differential loading increment is illustrated. It can be easily seen that, the resisting part $\dot{\epsilon}^f$ is just the strain increment that would produce the stress increment $\dot{\sigma}$ while the current secant compliance \mathbf{C} remains unchanged, i.e. the damage would not develop further, and correspondingly the degradation component $\dot{\epsilon}^d$ signify the strain increment that would be obtained while the current secant compliance \mathbf{C} increases under the current stress.

The degradation strain rate defined in Equation 8 first appeared in Hueckel & Maier (1977), and was later adopted by Ortiz (1985) and summarized in Carol et al. (1994).

2.3 Consistent projection operators

Just as pointed out in Mazars et al. (1990), the unilateral effects, i.e., the stiffness changes during the microcrack-closure-reopening (MCR) process, is of great significance for the modeling of concrete like quasi-brittle materials. To rationally describe the unilateral effects, many methods was proposed in the literature, while most continuum damage models adopt the spectral decomposition of a second-order tensors (the stress, the strain or effective stress) and introduce the fourth-order projection operators originated in Ortiz(1985) and later developed in Simo & Ju (1987) and Carol & Willam (1996).

Due to its concept simplicity, the method of introducing projection operators is also employed here. However, new thermodynamically consistent projection operators which guarantee zero energy dissipation and generation, are proposed herein. Correspondingly, the nominal Cauchy stress tensor $\boldsymbol{\sigma}$ is decomposed into its positive and negative components, i.e.

$$\boldsymbol{\sigma} = \boldsymbol{\sigma}^+ + \boldsymbol{\sigma}^- \quad (9)$$

where the positive and negative components $\boldsymbol{\sigma}^\pm$ are expressed as

$$\boldsymbol{\sigma}^+ = \sum_{i=1} \langle \sigma^{(i)} \rangle \mathbf{n}^{(i)} \otimes \mathbf{n}^{(i)}, \quad \boldsymbol{\sigma}^- = \boldsymbol{\sigma} - \boldsymbol{\sigma}^+ \quad (10)$$

which $\sigma^{(i)}$ is i^{th} eigenvalue of $\boldsymbol{\sigma}$ with the corresponding eigenvector represented by $\mathbf{n}^{(i)}$, and $\langle \cdot \rangle$ denotes the McAuley bracket. Introducing the the positive and negative projection operators \mathbf{P}^\pm originated in Ortiz (1985), Equation 10 can be rewritten into

$$\boldsymbol{\sigma}^\pm = \mathbf{P}^\pm : \boldsymbol{\sigma}, \quad \mathbf{P}^+ + \mathbf{P}^- = \mathbf{I} \quad (11)$$

where \mathbf{I} is the symmetric fourth-order identity tensor.

However, the expressions of \mathbf{P}^\pm are not unique, and to guarantee zero spurious energy dissipation or generation upon fixed damage (Carol & Willam 1996), only the ones satisfying the following condition

$$\dot{\mathbf{P}}^\pm : \boldsymbol{\sigma} = \mathbf{0} \quad (12)$$

can be used in the modeling of anisotropic degradation. Combining Equation 11 with Equation 12, yields

$$\mathbf{P}^\pm : \dot{\boldsymbol{\sigma}} = \dot{\boldsymbol{\sigma}}^\pm, \quad \mathbf{P}^+ + \mathbf{P}^- = \mathbf{I} \quad (13)$$

In another word, thermodynamically consistent projection operators are those specific expressions of \mathbf{P}^\pm which simultaneously satisfy the conditions expressed in Equations 11 and 13.

In Faria et al. (2000) and Wu et al. (2006) the following expressions which satisfy Equation 13, were derived

$$\mathbf{P}^+ = \sum_i H_\sigma^{(i)} \mathbf{N}^{(ii)} + \mathbf{T}, \quad \mathbf{P}^- = \mathbf{I} - \mathbf{P}^+ \quad (14)$$

where $H_\sigma^{(i)}$ denotes the Heaviside function of $\sigma^{(i)}$. In Equation 14, the symmetric fourth-order tensor \mathbf{T} is expressed as

$$\mathbf{T} = 2 \sum_{i=1, i>j} \frac{\langle \sigma^{(i)} \rangle - \langle \sigma^{(j)} \rangle}{\sigma^{(i)} - \sigma^{(j)}} \mathbf{N}^{(ij)} \quad (15)$$

where the fourth-order tensor $\mathbf{N}^{(ij)} = \mathbf{N}^{(ij)} \otimes \mathbf{N}^{(ij)}$ with the second-order symmetric tensor $\mathbf{N}^{(ij)}$ reading

$$\mathbf{N}^{(ij)} = \mathbf{N}^{(ji)} = \frac{1}{2} (\mathbf{n}^{(i)} \otimes \mathbf{n}^{(j)} + \mathbf{n}^{(j)} \otimes \mathbf{n}^{(i)}) \quad (16)$$

It is interesting to note that, the first term in Equation 14 is just the expression originated in Ortiz (1985), and one can easily verify that $\mathbf{T} : \boldsymbol{\sigma} = \mathbf{0}$. Also, it can be proved that, for a class of unified expressions of projection operators, Equation 14 is unique. Therefore, \mathbf{P}^\pm expressed in Equations 14–16 are also the projection operators of the stress $\boldsymbol{\sigma}$, i.e., they are thermodynamical consistent in concerned with the requirement of zero energy dissipation, and can be employed in the modeling of unilateral effects.

2.4 Considering unilateral effects

With the proposed consistent projection operators, the Gibbs free energy ψ considering the unilateral effects, is here defined similar to that originated in Ortiz (1985), i.e.

$$\begin{aligned} \psi &= \frac{1}{2} \boldsymbol{\sigma} : \mathbf{C} : \boldsymbol{\sigma} = \frac{1}{2} \boldsymbol{\sigma} : (\mathbf{C}_0 + \boldsymbol{\Lambda}^+ + \boldsymbol{\Lambda}^-) : \boldsymbol{\sigma} \quad (17) \\ &= \frac{1}{2} \boldsymbol{\sigma} : \mathbf{C}_0 : \boldsymbol{\sigma} + \frac{1}{2} \boldsymbol{\sigma}^+ : \bar{\boldsymbol{\Lambda}}^+ : \boldsymbol{\sigma}^+ + \frac{1}{2} \boldsymbol{\sigma}^- : \bar{\boldsymbol{\Lambda}}^- : \boldsymbol{\sigma}^- \end{aligned}$$

where $\boldsymbol{\Lambda}^\pm$ denote the increases of the actual compliances under general stress state, with expressions as

$$\boldsymbol{\Lambda}^\pm = \mathbf{P}^\pm : \bar{\boldsymbol{\Lambda}}^\pm : \mathbf{P}^\pm, \quad \boldsymbol{\Lambda} = \boldsymbol{\Lambda}^+ + \boldsymbol{\Lambda}^- \quad (18)$$

and $\bar{\Lambda}^\pm$ signify the increases of the intrinsic secant compliances under the purely positive and purely negative stresses, which are selected as the internal variables. Correspondingly, the secant strain–stress relation considering the unilateral effects is expressed as

$$\epsilon = \frac{\partial \psi}{\partial \sigma} = \mathbf{C} : \sigma, \quad \sigma = \mathbf{S} : \epsilon, \quad \mathbf{S} = \mathbf{C}^{-1} \quad (19)$$

where the secant compliance \mathbf{C} reads

$$\mathbf{C} = \mathbf{C}_0 + \mathbf{P}^+ : \bar{\Lambda}^+ : \mathbf{P}^+ + \mathbf{P}^- : \bar{\Lambda}^- : \mathbf{P}^- \quad (20)$$

Besides the above secant constitutive law, the second thermodynamics principle also leads to the following damage dissipation inequality

$$\dot{H} = (-\mathbf{Y}^+) :: \dot{\bar{\Lambda}}^+ + (-\mathbf{Y}^-) :: \dot{\bar{\Lambda}}^- \geq 0 \quad (21)$$

where the thermodynamical forces conjugate to the selected damage variables $\bar{\Lambda}^\pm$, i.e. the damage energy release rates $-\mathbf{Y}^\pm$ are expressed as

$$-\mathbf{Y}^\pm = \frac{\partial \psi}{\partial \bar{\Lambda}^\pm} = \frac{1}{2} \sigma^\pm \otimes \sigma^\pm \quad (22)$$

It is then appropriate that the evolution laws for the total added secant compliance is postulated resembling that for the plastic irreversible strains, i.e.

$$\dot{\bar{\Lambda}}^\pm = \dot{\lambda}^\pm \Psi^\pm \quad (23)$$

where, $\dot{\lambda}^\pm \geq 0$ denote the damage consistency parameters, and to inherently guarantee the non-negative of the overall damage dissipation, the evolution directions Ψ^\pm should be non-negative definite fourth-order symmetric tensors.

Therefore in Equation 8, the rate of secant compliance $\dot{\mathbf{C}}$ is expressed as

$$\dot{\mathbf{C}} = 2\mathbf{P}^+ : \dot{\bar{\Lambda}}^+ : \mathbf{P}^+ + 2\mathbf{P}^- : \dot{\bar{\Lambda}}^- : \mathbf{P}^- + \dot{\bar{\Lambda}}^+ + \dot{\bar{\Lambda}}^- \quad (24)$$

and the degradation strain rate $\dot{\epsilon}^d$ becomes

$$\dot{\epsilon}^d = (\dot{\lambda}^+ \Psi^+ + \dot{\lambda}^- \Psi^-) : \sigma = \dot{\lambda}^+ \Gamma^+ + \dot{\lambda}^- \Gamma^- \quad (25)$$

where, the evolution directions of the degradation strain Γ^\pm are expressed as

$$\Gamma^\pm = \Psi^\pm : \sigma \quad (26)$$

2.5 Continuum Tangent Stiffness

Neither the rate constitutive law nor the numerical consistent tangent modulus were derived in nearly all the anisotropic degradation models which introduced the projection operators to describe the unilateral effects. To the authors limit knowledge, only in

Mahnken et al. (2000) the implicit integration scheme and the consistent tangent modulus were obtained in concerned with the model of Ortiz (1985), however, the derivations were rather complex and the final expressions were terribly lengthy, comparing to the ones to be demonstrated as follows.

To determine the damage states, the following damage criterion F^\pm are postulated in terms of the stress σ and of the previous history r^\pm , i.e.

$$F^\pm(\sigma, r^\pm) = f^\pm(\sigma) - r^\pm(\lambda^\pm) \leq 0 \quad (27)$$

where damage thresholds r^\pm are functions of the cumulative damage measure $\lambda^\pm = \int_0^t \dot{\lambda}^\pm dt$, and the damage loading/unloading conditions can be expressed as

$$\dot{\lambda}^\pm \geq 0, \quad F^\pm \leq 0, \quad \dot{\lambda}^\pm F^\pm = 0 \quad (28)$$

Upon damage loading, i.e. $\dot{\lambda}^\pm > 0$, $\dot{\lambda}^\pm$ can be determined by the damage consistency conditions $\dot{F}^\pm = 0$, i.e.

$$\dot{F}^\pm = \mathbf{Y}^\pm : \dot{\sigma} - \dot{\lambda}^\pm h^\pm = 0 \quad (29)$$

where \mathbf{Y}^\pm denote the stress gradient of the damage criterion surfaces F^\pm , and h^\pm are the softening/hardening functions, respectively expressed as

$$\mathbf{Y}^\pm = \frac{\partial F^\pm}{\partial \sigma} = \frac{\partial f^\pm}{\partial \sigma}, \quad h^\pm = \frac{\partial F^\pm}{\partial \lambda^\pm} = \frac{\partial r^\pm}{\partial \lambda^\pm} \quad (30)$$

Calling for the relations presented in Equations 7 and 25, the damage consistency parameters $\dot{\lambda}^\pm$ can be obtained under different loading cases, and the rate form of the constitutive relation reads

$$\dot{\sigma} = \mathbf{S}^{\text{tan}} : \dot{\epsilon} \quad (31)$$

where the tangent stiffness \mathbf{S}^{tan} are expressed as

- If $F^+ < 0, F^- < 0$

$$\dot{\lambda}^+ = \dot{\lambda}^- = 0, \quad \mathbf{S}^{\text{tan}} = \mathbf{S} \quad (32)$$

- If $F^+ = \dot{F}^+ = 0, F^- < 0$

$$\dot{\lambda}^+ = \frac{\mathbf{Y}^+ : \mathbf{S} : \dot{\epsilon}}{h^+ + \mathbf{Y}^+ : \mathbf{S} : \Gamma^+}, \quad \dot{\lambda}^- = 0 \quad (33)$$

$$\mathbf{S}^{\text{tan}} = \mathbf{S} - \frac{\mathbf{S} : (\Gamma^+ \otimes \mathbf{Y}^+) : \mathbf{S}}{h^+ + \mathbf{Y}^+ : \mathbf{S} : \Gamma^+} \quad (34)$$

- If $F^+ < 0, F^- = \dot{F}^- = 0$

$$\dot{\lambda}^+ = 0, \quad \dot{\lambda}^- = \frac{\mathbf{Y}^- : \mathbf{S} : \dot{\epsilon}}{h^- + \mathbf{Y}^- : \mathbf{S} : \Gamma^-} \quad (35)$$

$$\mathbf{S}^{\text{tan}} = \mathbf{S} - \frac{\mathbf{S} : (\Gamma^- \otimes \mathbf{Y}^-) : \mathbf{S}}{h^- + \mathbf{Y}^- : \mathbf{S} : \Gamma^-} \quad (36)$$

- If $F^+ = \dot{F}^+ = 0, F^- = \dot{F}^- = 0$

$$\begin{bmatrix} \dot{\lambda}^+ \\ \dot{\lambda}^- \end{bmatrix} = \frac{1}{\Delta} \begin{bmatrix} (h_{22} \mathbf{Y}^+ - h_{12} \mathbf{Y}^-) : \mathbf{S} : \dot{\epsilon} \\ (h_{11} \mathbf{Y}^- - h_{21} \mathbf{Y}^+) : \mathbf{S} : \dot{\epsilon} \end{bmatrix} \quad (37)$$

$$\begin{aligned} \mathbf{S}^{\text{tan}} = \mathbf{S} - \frac{1}{\Delta} \mathbf{S} : & \left[\mathbf{\Gamma}^+ \otimes (h_{22} \mathbf{Y}^+ - h_{12} \mathbf{Y}^-) \right. \\ & \left. + \mathbf{\Gamma}^- \otimes (h_{11} \mathbf{Y}^- - h_{21} \mathbf{Y}^+) \right] : \mathbf{S} \end{aligned} \quad (38)$$

with the factors h_{ij} and Δ respectively expressed as

$$\begin{aligned} h_{11} &= h^+ + \mathbf{Y}^+ : \mathbf{S} : \mathbf{\Gamma}^+, & h_{12} &= \mathbf{Y}^+ : \mathbf{S} : \mathbf{\Gamma}^- \\ h_{21} &= \mathbf{Y}^- : \mathbf{S} : \mathbf{\Gamma}^+, & h_{22} &= h^- + \mathbf{Y}^- : \mathbf{S} : \mathbf{\Gamma}^- \\ \Delta &= h_{11}h_{22} - h_{12}h_{21} \end{aligned} \quad (39)$$

Noted that, the tangent stiffness will be generally asymmetric unless the associated evolution laws for the degradation strain (i.e. $\mathbf{Y}^\pm = \mathbf{\Gamma}^\pm$) are adopted.

Equations 32–38 actually constitute the classical problem of multisurface degradation, which is readily solved by the standard multisurface return mapping integration algorithm (Simo & Hughes 1998).

3 APPLICATION TO CONCRETE MODELING

In this section, the above proposed stress-based elastic anisotropic unilateral degradation model is applied to capture the typical nonlinear features of concrete, by specialization of the presented formulations.

3.1 Damage evolution laws

Concrete is known to behave as a quasi-brittle material that contains numerous microcracks and microvoids. From experimental observations, damage in concrete is inherently an anisotropic and continuous process that initiates at very low level of the applied loading. Here, the evolution directions for the intrinsic added secant compliances Λ^\pm are postulated as

$$\Psi^\pm = \frac{1}{E_0} \left[(1 + \nu_0) \mathbf{I}_\sigma^\pm \otimes \underline{\underline{\mathbf{I}}}_\sigma^\pm - \nu_0 \mathbf{I}_\sigma^\pm \otimes \mathbf{I}_\sigma^\pm \right] \quad (40)$$

Correspondingly, one obtains

$$\mathbf{\Gamma}^\pm = \frac{1}{E_0} \left[(1 + \nu_0) (\mathbf{I}_\sigma^\pm)^2 - \nu_0 \mathbf{I} \right] \cdot \boldsymbol{\sigma}^\pm \quad (41)$$

where second-order tensors $\mathbf{I}_\sigma^\pm = \boldsymbol{\sigma}^\pm / \sqrt{\boldsymbol{\sigma}^\pm : \boldsymbol{\sigma}^\pm}$ are the unit tensors of $\boldsymbol{\sigma}^\pm$.

The evolution laws for the damage thresholds r^\pm can be determined by mapping the proposed constitutive law into the uniaxial stress states. Considering that the amount of damage that takes place at very low

stress levels may be considered insignificant and significant damage appears only beyond a certain stress threshold, the following functions are postulated in this contribution for the damage thresholds r^\pm

$$r^+ = \frac{f_0^+}{(1 + \lambda^+)^{\tilde{a}^+}}, \quad r^- = \frac{1 + \tilde{a}^- \ln(1 + \lambda^-)}{1 + \lambda^-} f_0^- \quad (42)$$

where \tilde{a}^\pm are the parameters respectively controlling the softening/hardening shapes of the obtained uniaxial stress-strain curves; f_0^\pm are the elastic limit strengths (positive values) upon which the nonlinearity under uniaxial tensile and compressive states become evident, are respectively expressed as

$$f_0^+ = f_t, \quad f_0^- = \frac{1}{\tilde{a}^-} f_c \exp\left(1 - \frac{1}{\tilde{a}^-}\right) \quad (43)$$

with f_t and f_c denoting the uniaxial tensile and compressive strengths.

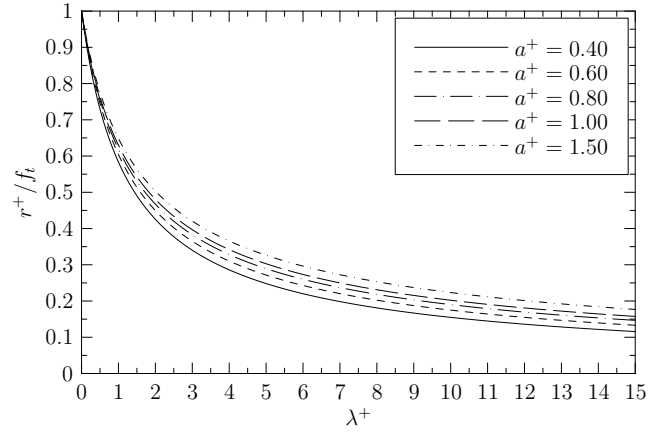


Figure 2: Positive threshold-cumulative damage curves for variable values of a^+ .

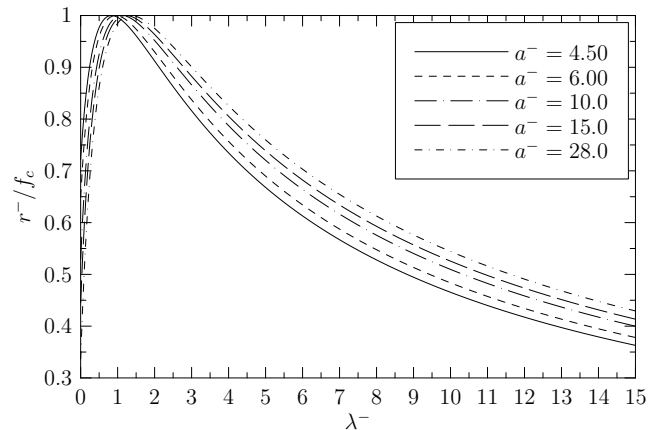


Figure 3: Negative threshold-cumulative damage curves for variable values of a^- .

To be used in the post-peak nonlinear finite element computations of concrete structures, the above evolution laws for r^\pm have to be regularized either employing the crack band theory (Bazant & Oh 1983), the

non-local methods (Bazant & Pijaudier-Cabot 1988) or the gradient models (de Borst et al. 1995). If the crack band theory is adopted, parameters \tilde{a}^\pm should be determined in terms of the Mode-I and Mode-II fracture energies per unit volume G_f^+/l_{ch} and G_f^-/l_{ch} , with l_{ch} denoting the characteristic length of the finite element. By integrating the area under the uniaxial tensile and compressive stress–strain curves (refer to Section 3.3), one obtains

$$\tilde{a}^+ = \frac{a^+ + 1}{2a^+ + 1}, \quad \tilde{a}^- = \frac{\sqrt{1 + 8a^-} - 1}{2} \quad (44)$$

$$a^\pm = \left[\frac{G_f^\pm E_0}{l_{ch}(f_0^\pm)^2} - \frac{1}{2} \right] > 0 \quad (45)$$

The evolution laws for the damage thresholds r^\pm represented against with the cumulative damages λ^\pm for variable values of a^\pm are illustrated in Figure 2 and 3.

3.2 Loading functions

For concrete like quasi-brittle materials the following damage loading functions f^\pm are adopted

$$f^+(\boldsymbol{\sigma}) = (\boldsymbol{\sigma}^+ : \boldsymbol{\Theta}^+ : \boldsymbol{\sigma}^+)^{\frac{1}{2}} \quad (46a)$$

$$f^-(\boldsymbol{\sigma}) = (\boldsymbol{\sigma}^- : \boldsymbol{\Theta}^- : \boldsymbol{\sigma}^- + c^2 \boldsymbol{\sigma}^+ : \boldsymbol{\Theta}^+ : \boldsymbol{\sigma}^+)^{\frac{1}{2}} \quad (46b)$$

where the parameter $c = \sqrt{3}f_c/(2f_t)$ is introduced to describe the cross “tensile-compressive softening” effect of the tensile stress on the lateral compressive nonlinearity, and the two symmetric isotropic fourth-order tensors $\boldsymbol{\Theta}^\pm$ are expressed

$$\boldsymbol{\Theta}^\pm = (1 + v^\pm) \mathbf{I} \otimes \mathbf{I} - v^\pm \mathbf{I} \otimes \mathbf{I} \quad (47)$$

with two parameters v^\pm determined as follows.

Denoted the strength under equi-biaxial tension by f_{bt} , the following relation can be obtained

$$f_t = \sqrt{2(1 - v^+)} f_{bt} \implies f_{bt} = \frac{f_t}{\sqrt{2(1 - v^+)}} \quad (48)$$

It is obvious that, if v^+ takes the value of the Poisson’s ratio (between 0.15 and 0.25), f_{bt}/f_t lies in the ranges of 0.767–0.816, which fits the test data (Kupfer et al. 1969) very well. Therefore, if there is no support of experimental data, $v^+ = \nu_0$ and $\boldsymbol{\Theta}^+ = E_0 \cdot \mathbf{C}_0$ can be adopted.

Similarly, if the strength (positive value) under equi-biaxial compression are signified by f_{bc} , one obtains

$$f_c = \sqrt{2(1 - v^-)} f_{bc} \implies v^- = 1 - \frac{1}{2} \left(\frac{f_c}{f_{bc}} \right)^2 \quad (49)$$

From the test data of typical concrete material, the ratio of f_{bc}/f_c generally ranges in 1.10–1.20 (Kupfer et al. 1969), which leads to v^- lying between 0.587 and 0.653. In the present paper, the value of f_{bc}/f_c is taken as 1.16, implying that $v^- = 0.6284$.

3.3 Application examples

In this subsection, the numerical concrete tests with the material properties of $E_0 = 3.0 \times 10^4 \text{MPa}$, $\nu_0 = 0.20$, $f_t = 3.0 \text{MPa}$, $f_c = 30.0 \text{MPa}$, and $f_{bc}/f_c = 1.16$, are analyzed.

Firstly, considering the uniaxial tension ($\sigma_1 > 0, \sigma_2 = \sigma_3 = 0$), i.e. all the other components of $\bar{\boldsymbol{\Lambda}}^\pm$ are zero only except the non-zero component $\bar{\Lambda}_{1111}^+ = \lambda^+/E_0$, we obtain the stress-strain relation can be expressed as

$$\sigma_1 = \begin{cases} f_0^+ \tilde{\epsilon}_0^+ & (0 \leq \tilde{\epsilon}_0^+ \leq 1.0) \\ f_0^+ \left(\frac{1}{\tilde{\epsilon}_0^+} \right)^{1+\frac{1}{a^+}} & (\tilde{\epsilon}_0^+ \geq 1.0) \end{cases} \quad (50)$$

where, the normalized strain $\tilde{\epsilon}^+$ is expressed

$$\tilde{\epsilon}_0^+ = \frac{\epsilon_1}{\epsilon_0^+}, \quad \epsilon_0^+ = \frac{f_0^+}{E_0} \quad (51)$$

The above stress-strain diagram is illustrated in Figure 4 for different values of a^+ . It is apparent that, for the higher value of parameter a^+ , the decays of σ_1 are the slower, while for progressively lower finite values of a^+ , softening is more pronounced.

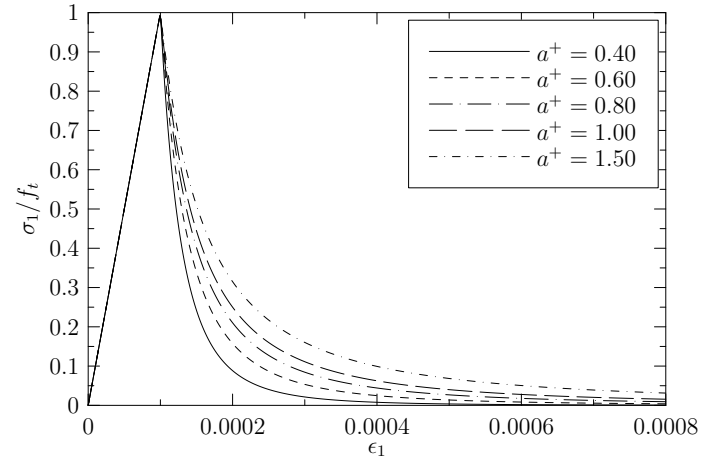


Figure 4: Uniaxial tensile stress-strain curves for different values of a^+ .

Secondly, under the uniaxial compression ($\sigma_1 = \sigma_2 = 0, \sigma_3 < 0$), all the other components of $\bar{\boldsymbol{\Lambda}}^\pm$ will be zero only except the non-zero component $\bar{\Lambda}_{3333}^- = \lambda^-/E_0$. Under such condition, the uniaxial compressive stress-strain relation can also be obtained as

$$\sigma_3 = \begin{cases} f_0^- \tilde{\epsilon}_0^- & (0 \leq \tilde{\epsilon}_0^- \leq 1.0) \\ f_0^- \tilde{\epsilon}_0^- \exp \left(\frac{1 - \tilde{\epsilon}_0^-}{\tilde{a}^-} \right) & (1.0 \leq \tilde{\epsilon}_0^-) \end{cases} \quad (52)$$

where the negative normalized strain under uniaxial compression is represented by

$$\tilde{\epsilon}_0^- = \frac{\epsilon_3}{\epsilon_0^-}, \quad \epsilon_0^- = \frac{f_0^-}{E_0} \quad (53)$$

The obtained stress-strain relation for different values of a^- is then illustrated in Figure 5. It can be seen that, the higher value parameter a^- takes, the slower the decays of σ_3 are.

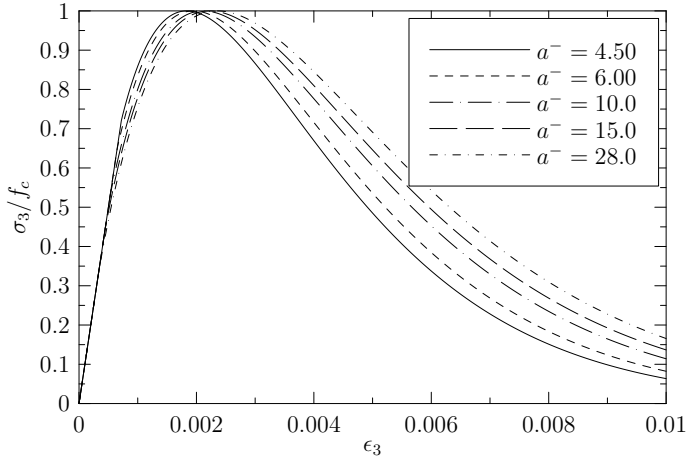


Figure 5: Uniaxial compressive stress-strain curves for different values of a^- .

The evolution of cyclic stress $\sigma_1 = \sigma_{xx}$ along the loading direction x against the prescribed strain ϵ_1 (O \rightarrow A \rightarrow B \rightarrow O \rightarrow C \rightarrow D \rightarrow O \rightarrow B \rightarrow E \rightarrow O), is illustrated in Figure 6, with parameters of $a^+ = 0.50$, $a^- = 6.00$. It is clearly seen that, the stiffness degradation and the unilateral effect during the microcracks closure-reopening, can be well described by the proposed model.

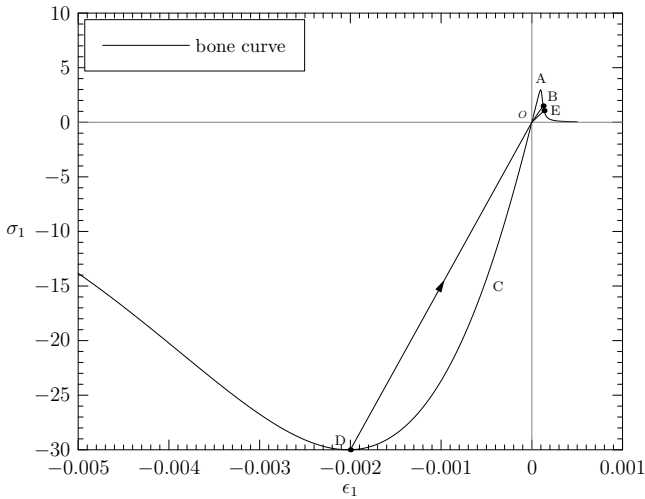


Figure 6: Stress-strain curves under cyclic uniaxial tension-compression.

Finally, the obtained strength envelope under biaxial stress states ($\sigma_2 = 0$) is referred to Figure 7 which agrees fairly well with the one obtained from the experimental data (Kupfer et al. 1969): not only the strength enhancements under biaxial compressive confinement, but also the strength decays due to the lateral tensile stresses, can be well predicted by the proposed model.

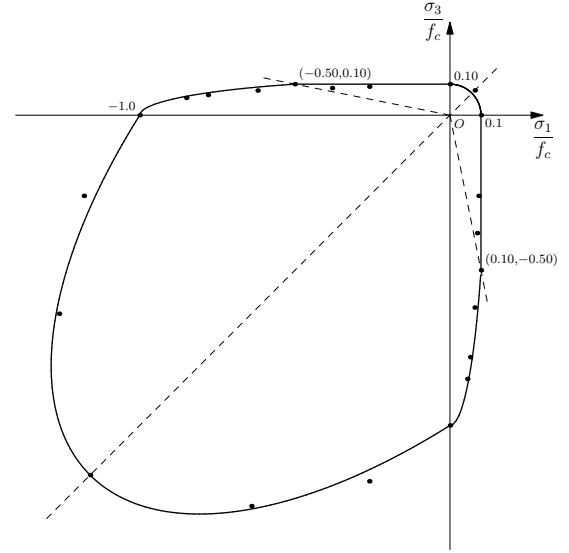


Figure 7: Strength envelope obtained under biaxial stress.

In above illustrative applications, the predicted damages evolve only in the loading directions and the damages in the lateral perpendicular directions remain zero. However, for an isotropic damage model the damages in all the directions will be same. Therefore, though the uniaxial and biaxial applications are very simple, they actually demonstrate the capability of the proposed elastic anisotropic degradation unilateral model for describing most of the nonlinear performances of concrete, such as strength softening, stiffness degradation, decays of compressive strength due to the lateral tensile stress, strength and ductility enhancement under lateral compressive confinement, unilateral effects and damage induced anisotropy, etc.

4 CONCLUSIONS

In this contribution a thermodynamically consistent stress-based elastic anisotropic degradation unilateral model is proposed and then applied to concrete modeling. The increases of the intrinsic secant compliance under the purely positive and purely negative stresses are adopted as the internal damage variables, and therefore the hypothesis of strain equivalence or strain energy equivalence is no longer required. To consider the unilateral effects, new consistent positive and negative projection operators are proposed, and the secant constitutive law is then established within the framework of irreversible thermodynamics. The rate formulations and the corresponding tangent stiffness are also derived, which can be employed to develop standard structure of the classical multisurface return mapping integration algorithm. Finally, the proposed model is verified by application to concrete modeling.

The numerical algorithm, and more complex applications, e.g. the Willam's test (Willam et al. 1987), the mixed fracture controlled tests of Nooru-Mohamed, Hassanzadeh and others (di Prisco et al. 2000), will be discussed later.

REFERENCES

- [1] Bazant, Z.P. & Oh, B. 1983. Crack band theory for fracture of concrete. *RILEM Material of Structure*, 16:155-77.
- [2] Bazant, Z.P. & Pijaudier-Cabot, G. 1988. Nonlocal continuum damage, localization instability and convergence. *ASME Journal of Applied Mechanics*, 55: 287-293.
- [3] Carol, I., Rizzi, E. & Willam, K. 1994. A unified theory of elastic degradation and damage based on a loading surface. *International Journal of Solids and Structures*, 31(20): 2835-2865.
- [4] Carol, I. & Willam, K. 1996. Spurious energies dissipation/generation in stiffness recovery models for elastic degradation and damage. *International Journal of Solids and Structures*, 33(20-22): 2939-2957.
- [5] Carol, I., Rizzi, E. & Willam, K. 2001. On the formulation of anisotropic elastic degradation. I: Theory based on a pseudo-logarithmic damage tensor rate; II: Generalized pseudo-Rankine model for tensile damage. *International Journal of Solids and Structures*, 38(4): 491-546.
- [6] Cordebois, J.P. & Sidoroff, F. 1979. Damage-induced elastic anisotropy. In Jean-Paul Boehler (ed.), *Mechanics of Behavior of Anisotropic Solids/No.295 Comportement Mécanique Des Solides Anisotropes*: 19-22. Martinus: Nijhoff Publisher.
- [7] de Borst, R. et al. 1995. On gradient-enhanced damage and plasticity models for failure in quasi-brittle and frictional materials. *Computational Mechanics*, 17: 130-141.
- [8] di Prisco, M., et al. 2000. Mixed mode fracture in plain and reinforced concrete: some results on benchmark tests. *International Journal of Fracture*, 103: 127-148.
- [9] Faria, R., Oliver, J. & Cervera, M. 2000. On isotropic scalar damage models for the numerical analysis of concrete structures. *CIMNE Monograph*, No.198. Barcelona, Spain.
- [10] Govindjee, S., Kay, G.J. & Simo, J.C. 1995. Anisotropic modeling and numerical simulation of brittle damage in concrete. *International Journal for Numerical Methods in Engineering*, 38(21): 3611-3634.
- [11] Hansen, E., Willam, K. & Carol, I. 2001. A two-surface anisotropic damage/plasticity model for plain concrete. In: R. de Borst (ed.), *Proceedings of Francos-4 Conference*, Paris, France.
- [12] Hueckel, T. & Maier, G. 1977. Incrementally boundary value problems in the presence of coupling of elastic and plastic deformations: A rock mechanics oriented theory. *International Journal of Solids and Structures*, 13: 1-15.
- [13] Ju, J. W. 1989. On energy-based coupled elastoplastic damage theories: Constitutive modeling and computational aspects. *International Journal of Solids and Structures*, 25(7): 803-833.
- [14] Kachanov, L.M. 1958. Time rupture process under creep conditions. *Izv. A Rad. Nauk. SSSR otd Tekh. Nauk*, 8: 26-31 (in Russian).
- [15] Krajcinovic, D. 2003. *Damage mechanics*. Amsterdam, Netherland: Elsevier.
- [16] Kupfer, H., Hilsdorf, H.K. & Rush, H. 1969. Behavior of concrete under biaxial stress. *ACI Journal*, 66: 656-666.
- [17] Lemaitre, J. 1971. Evaluation of dissipation and damage in metals. *Proc. I.C.M* : 1. Kyoto, Japan.
- [18] Mahnken, D., Tikhomirov, D. & Stein, E. 2000. Implicit integration scheme and its consistent linearization for an elastoplastic-damage model with application to concrete. *Computers and Structures*, 75: 135-143.
- [19] Mazars, J., Berthaud, Y. & Ramtani, S. 1990. The unilateral behaviour of damaged concrete. *Engineering Fracture Mechanics*, 35: 629-635.
- [20] Meschke, G, Lackner, R. & Mang, H.A. 1998. An anisotropic elastoplastic-damage model for plain concrete. *International Journal for Numerical Methods in Engineering*, 42: 703-727.
- [21] Neilsen, M.K. & Schreyer, H.L. 1992. Bifurcations in elastic-damaging materials. In J.Y. Ju and K.C. Valanis(eds.), *Damage Mechanics and Localization ASME*, AMD-Vol.142, MD-Vol.34: 109-123.
- [22] Ortiz, M. 1985. A constitutive theory for inelastic behaviour of concrete. *Mechanics of Materials*, 4: 67-93.
- [23] Simo, J. C. & Hughes, T. J. R. 1998, *Computational Inelasticity*. New York: Springer-Verlag.
- [24] Simo, C. & Ju, J.W. 1987. Stress and strain based continuum damage models. I: Formulation; and II: Computational aspects. *International Journal of Solids and Structures*, 23: 375-400.
- [25] Willam, K., Pramono, E. & Sture, S. 1987. Fundamental issues of smeared crack models. In S.P. Shah, and S.E. Swartz (eds.), *SEM/RILEM, Int. Conf. on Fracture of Concrete and Rock*: 192-207. Bethel, Connecticut: Society of Engineering Mechanics.
- [26] Wu, J.Y., Li, J. & Faria, R. 2006. An energy release rate-based plastic-damage model for concrete. *International Journal of Solids and Structures*, 43(3-4): 583-612.
- [27] Yazdani, S. & Schreyer, H.L. 1990. Combined plasticity and damage mechanics model for plain concrete. *Journal of Engineering Mechanics*, ASCE, 116: 1435-1450.